What do Ab Initio Calculations Predict for the Structure of Lithiated Azaenolates of Peptides?

Martin Feigel,* Gisela Martinek, and Wolfgang H. B. Sauer

Abstract: Structures and conformations of the azaenolate lithium salts of amides (formamide, acetamide, and *N*-methylacetamide) and of the dipeptide model *N*-formylalaninamide were investigated by means of ab initio MO theory. Four possible structures of the lithiated *C*-enolates of acetamide were also included in the study. All structures were calculated at the HF/6-31+G(d) and MP2(fc)/6-31+G(d)//HF/6-31+G(d) levels; the lithiated azaenolates of formamide were also investigated at higher theoretical levels (up to MP4(fc)/6-311+G(d,p)//MP2(fc)/6-311+G(d,p)). For the lithiated azaenolates of all amides investigated, the most stable structure contains a four-membered ring in which the lithium ion is complexed by the oxygen and nitrogen atoms; the substituents attached to the carbon and nitrogen atoms of the azaenolate are in a *cis* arrangement. The lithiated azaenolates of acetamide are predicted to be more stable than the corresponding *C*-enolates. To simulate solvation, calculations on complexes of the lithiated azaenolates of formamide with up to three molecules dimethyl ether were also performed, and all azaenolates of amides were also reoptimized by ab initio reaction-field calculations. Both solvation models reduce the preference for lithium-chelated *cis* structures. The Ramachandran maps of the dilithiated bis(azaenolate) of *N*-formylalaninamide (having *cis* or *trans* arrangements of the azaenolate substituents) were scanned by MNDO calculations for conformational accessible regions. Thirteen stable structures were subsequently optimized at the HF/6-31+G(d) ab initio level. The global minimum resembles a peptide in C_7 conformation, but other conformations, not known for peptides, are close in energy. The structures of dimers of the lithiated azaenolates of *N*-methylacetamide and of glycinaldehyde were also calculated. The NMR chemical shielding of carbon, nitrogen, and oxygen atoms in all structures were predicted ab initio by using the gauge-including atomic orbital (GIAO) method.

Keywords
ab initio calculations · azaenolates · NMR chemical shifts · peptides · Ramachandran maps

Strong organolithium bases are able to remove the amide protons of peptides to form lithiated azaenolates (Scheme 1). Poly(azaenolates) can even be produced from peptides or cyclopeptides with an excess of the base.[1] The compounds are soluble in organic solvents such as tetrahydrofuran, especially if the solution contains additional lithium salts. Azaenolates are probably also present when polylithiated peptides containing a glycine or sarcosine residue are quenched with electrophiles giving stereospecific *C*-alkylation.[1-3] The reduction of cyclopeptides with a large excess of lithium aluminum hydride in THF[4] is another example where soluble poly(azaenolate)s may be involved. To predict the course and stereochemistry of their reactions, the shape and spatial arrangement of the lithiated peptides containing *C*- and *N*-enolates must be known. Unfortunately, the conformations of peptides containing enolates have not yet been determined by experiment. Only a few solid-state structures of the lithium salts of amides have been published.[5]

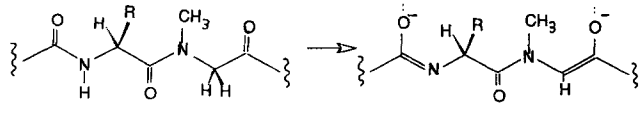

Scheme 1.

The present theoretical study investigates the azaenolate segment of small lithiated peptides. The aim of the work is to find the dominant stereochemical structures in lithiated azaenolates. We do not intend to explain the stereochemical outcome of a specific *C*-alkylation of a polylithiated peptide. We will rather explore the basic principles that define the structure of small peptidic azaenolates.

Even the relative energies of the (*E*) and (*Z*) geometries in lithiated azaenolates are unknown (Scheme 2). The azaenolate group will probably influence the preferred torsional angles ϕ and ψ in a peptide chain, and coordinating solvents (e.g., tetrahydrofuran) the relative energies of the structures. Furthermore, lithiated peptides are expected to aggregate; a number of dimers formed by azaenolates are compared in this study to

[*] Dr. M. Feigel,[+] Dr. W. H. B. Sauer, G. Martinek
Institut für Organische Chemie, Universität Erlangen-Nürnberg
Henkestr. 42, D-91054 Erlangen (Germany)
[+] New address: Fakultät für Chemie
Ruhr-Universität Bochum, D-44780 Bochum (Germany)
Telefax: Int. code + (234) 709-4479

  0947-6539/96/0201-0009 $ 10.00+.25/0

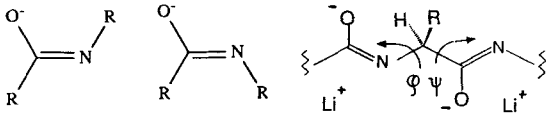

(Z), trans (E), cis

Scheme 2.

peptidic structures containing hydrogen bonds, for example, β-sheets. More complicated aggregates mixed with additional lithium salts or bases are presumably present under the experimental conditions of the alkylation experiments.[1-3]

The lithiated azaenolates **1**, **2**, and **3**, derived from formamide, acetamide, and *N*-methylacetamide, respectively, serve in the present computational study as small models to investigate whether an azaenolate preferentially adopts a *cis* [(*E*)-**1**, (*E*)-**2**, and (*E*)-**3**] or *trans* geometry [(*Z*)-**1**, (*Z*)-**2**, and (*Z*)-**3**] in the peptide. The quality of the calculations is checked for **1** by using different computational methods. The possible structures of the lithiated *C*-enolate of acetamide **4** are compared to those of the corresponding azaenolate **2**. Dilithiated *N*-formylalaninamide (**5**) is chosen to reflect the conformational preferences at the angles ϕ and ψ within a small peptide fragment. A number of systems are also investigated where lithium ions bridge the azaenolate moieties of two peptide chains.

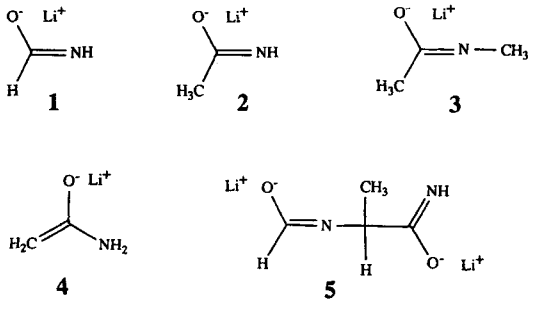

Results and Discussion

Lithiated azaenolates of formamide (1), acetamide (2), and *N*-methylacetamide (3): The structures **1A**, **1B**, and **1C** of *N*-lithiated formamide (Scheme 3) are related to the azaenolates of lithiated peptides.[6] The form **1A** is a model for the lithiated *cis* peptide bond, and structures **1B** and **1C** correspond to *trans* peptides with the lithium ion coordinated at the N and O atoms, respectively. The relative energies of these forms, established semiempirically (MNDO[7]) and by ab initio (G92[8]) calculations, are depicted in Figure 1.

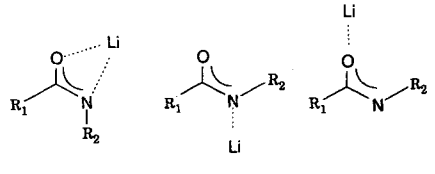

$R_1 = R_2 = H$	**1A**	**1B**	**1C**
$R_1 = CH_3$, $R_2 = H$	**2A**	**2B**	**2C**
$R_1 = R_2 = CH_3$	**3A**	**3B**	**3C**

Scheme 3.

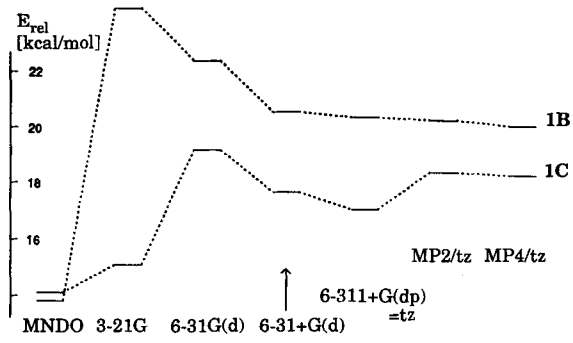

Fig. 1. Computational methods determine the relative energies of the lithiated azaenolates **1B** and **1C** relative to **1A** (H_f(MNDO), E(G92), kcal mol^{-1}). All structures were optimized at the indicated levels except the MP4/tz entry. Abbreviations: MP2/tz = MP2(fc)/6-311+G(d,p); MP4/tz = MP4(fc)/6-311+G(d,p)//MP2(fc)/6-311+G(d,p). The relative energies change by a maximum of 0.1 kcal mol^{-1} when an all-electron correlation, MP2(full)/6-31G(d), is used instead of MP2(fc)/6-31G(d) (not shown).

The most stable structure at all computational levels used is clearly **1A** (Fig. 1). Even MNDO favors **1A**, but the calculated energy differences to **1B** and **1C** are small compared to those obtained in the ab initio calculations. The most stable forms of the lithiated azaenolates of acetamide and *N*-methylacetamide are also the *cis* structures (**2A** and **3A**, respectively). The 6-31+G(d) optimized structures of **1**, **2**, and **3** are shown in Figures 2–4, respectively, and the energies are compiled in the Table 1. The lithium cation coordinates simultaneously to the carbonyl oxygen and to the amide nitrogen in the *cis* isomers. In contrast, only one coordination site can be accessed by lithium in the *trans* isomers, which are 14.5 to 22.0 kcal mol^{-1} less stable than the *cis* isomers. The carbonyl oxygen clearly binds lithium more effectively than the nitrogen ligand (compare the energy of the *trans* structures **1C**, **2C**, and **3C** to **1B**, **2B**, and **3B**).

The preference for the *cis* geometry, found in all lithiated azaenolates (Figs. 2–4), is presumably determined by lithium

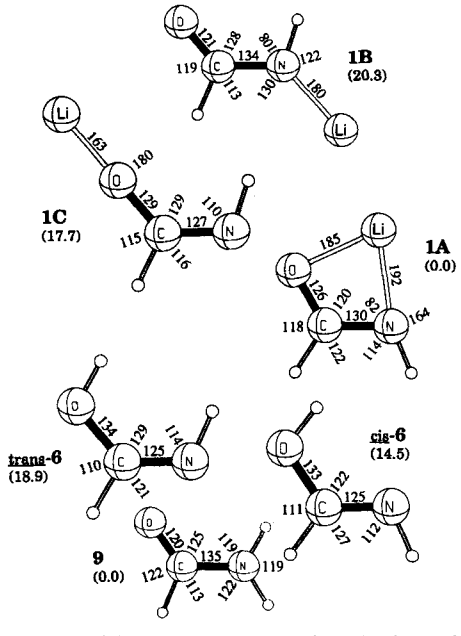

Fig. 2. Structures of formamide **9** and the corresponding azaenols *cis*-**6** and *trans*-**6** and lithiated azaenolates **1A**, **1B**, and **1C**. All structures are minima of C_s symmetry in the HF/6-31 + G(d) calculations. Relative energies (RHF/6-31 + G(d), kcal mol^{-1}) in the lithiated and the protonated group of isomers are given in parentheses.

0947-6539/96/0201-0010 $ 10.00+.25/0 Chem. Eur. J. 1996, 2, No. 1

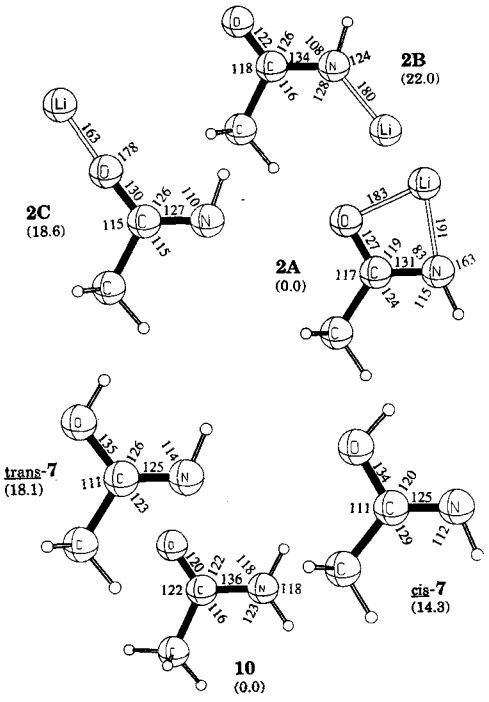

Fig. 3. Structures of acetamide **10** and the corresponding azaenols *cis*-**7** and *trans*-**7** and lithiated azaenolates **2A**, **2B**, and **2C**. The structures are minima in HF/6-31+G(d) calculations (acetamide **10** has C_1 symmetry, the other structures have C_s symmetry). Relative energies (HF/6-31+G(d), kcal mol^{-1}) in the lithiated and the protonated group of isomers are given in parentheses.

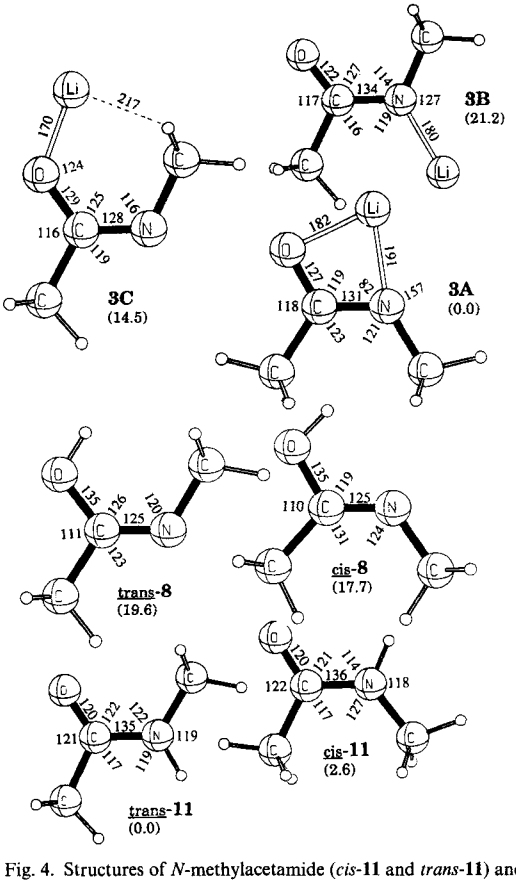

Fig. 4. Structures of *N*-methylacetamide (*cis*-**11** and *trans*-**11**) and the corresponding azaenols *cis*-**8** and *trans*-**8** and lithiated azaenolates **3A**, **3B**, and **3C**. The structures are minima in HF/6-31+G(d) calculations (*cis*-**11** has C_1 symmetry, the other structures have C_s symmetry. Relative energies (HF/6-31+ G(d), kcal mol^{-1}) in the lithiated and the protonated group of isomers are given in parentheses.

Table 1. Relative energies (kcal mol^{-1}) of different azaenolate forms of lithiated formamide (**1A–C**), acetamide (**2A–C**), and *N*-methylacetamide (**3A–C**), calculated by different methods. The lithiated structures of the *C*-enolate of acetamide **4A–D** are also listed. Dimethyl ether ligands are used to model the first solvation shell of **1A–C** in solution. All structures were exposed to a continuum reaction field and reoptimized to simulate solvation (SCRF). Representative structures are shown in the Figures 2–4, 6, and 5.

Structure	MNDO	HF/6-31+G(d)	MP2 [a]	MP2/ZPE [b]	SCRF [c]
1A	0.0	0.0	0.0	0.0	0.0
1B	13.8	20.6	20.3	19.9	−0.1
1C	14.1	17.7	18.4	17.4	0.2
1A·Me_2O	0.0	0.0	0.0	0.0	0.0
1B·Me_2O	11.7	17.0	17.7	17.8	1.1
1C·Me_2O	12.8	14.8	16.1	15.8	1.9
1A·2Me_2O	0.0	0.0	0.0	0.0	0.0
1B·2Me_2O	9.2	12.7	14.4	14.4	2.0
1C·2Me_2O	10.9	10.4	12.8	12.6	1.2
1A·3Me_2O	0.0	0.0	0.0	0.0 [d]	0.0
1B·3Me_2O	3.1	8.5	10.1	10.0 [d]	1.4
1C·3Me_2O	3.5	4.8	6.9	6.8 [d]	−0.4
2A	0.0	0.0	0.0	0.0	0.0
2B	10.1	22.0	21.5	21.0	6.9
2C	14.6	18.6	18.7	18.5	5.8
4A	10.4	25.9	24.2	23.7	26.0
4B	18.7	29.2	27.1	27.2	23.5
4C	24.7	33.0	34.0	33.5	24.9
4D	11.6	40.6	36.5	36.1	32.9
3A	0.0	0.0	0.0	0.0	0.0
3B	9.5	21.2	20.5	20.0	9.9
3C	9.2	14.5	13.5	13.2	6.6

[a] MP2(fc)/6-31+G(d)//6-31+G(d). [b] MP2 value in column three corrected by the zero-point energy from frequency calculations at the HF/6-31+G(d) level. [c] Reaction-field calculations with the dielectric constant of THF at HF/6-31+G(d). The cavity size has been adjusted after the first SCRF geometry optimization to accommodate for the movements of the lithium cation. The change in the cavity radius in this procedure was significant with up to 7 pm in the different forms **1A–C** of lithiated formamide. [d] The zero-point correction of these large systems is based on calculations at the 3-21G level; all other frequencies were calculated with the 6-31+G(d) basis.

complexation. The parent azaenols **6**, **7**, and **8** (the tautomers of formamide, acetamide, and *N*-methylacetamide, respectively) also prefer the *cis* arrangement (see Figs. 2–4), but the energy differences to the less stable *trans* structures are very small (1.8–4.4 kcal mol^{-1}) compared to the differences found in the lithiated systems. Calculations on the non-lithiated azaenolate anions confirm that lithium coordination determines the *cis*/*trans* ratio: The energetic order of *cis* and *trans* structures is reversed in the free anions—the *trans* form is calculated to be around 6 kcal mol^{-1} more stable than the *cis* form.[9]

The geometries of the lithium azaenolates may be compared to those of the corresponding protonated azaenolates (the *cis*- and *trans*-azaenols **6**, **7**, and **8**) and to those of formamide (**9**), acetamide (**10**), and *N*-methylacetamide (*cis*-**11**, *trans*-**11**) (Figs. 2–4). They were calculated at the same level of theory as that used for the lithium systems.[10] The *N*-lithiated *trans*-azaenolates **1B**, **2B**, and **3B** are obviously structurally related to their amide precursors (**9**, **10**, and *trans*-**11**). The C–N and C=O bond lengths change very little (±2 pm) on going from the amide to the lithiated system. A simple interpretation is that the lithium ion in **1B**, **2B**, and **3B** localizes the negative charge at nitrogen so that the amide bond system remains untouched. This is supported by a natural bond orbital (NBO) analysis[13] of the 6-31+G(d) results: the Wiberg bond indices of the C–N bonds (calculated in the NAO basis by L607 of Gaussian 92[8]) are comparable in the azaenolate **1B** and in the amide **9** (1.32 and 1.17, indicating partial double-bond character). However, coordination of the lithium cation at the oxygen of an azaenolate (e.g., in **1C**) increases the index to 1.8; the C–N bond can

therefore reasonably be described as being a formal double bond. The charge localization is reflected in the natural population analysis (NPA): Both systems, **1B** and **1C**, are described here as being contact ion pairs between a lithium cation and the azaenolate anion, but the position of the lithium ion determines the electron distribution in the anion. Lithium coordination at the nitrogen polarizes the anion toward N (NPA charges in **1B**: N, −1.29; O, −0.78), coordination at the oxygen localizes more charge at O (NPA charges in **1C**: N, −0.87; O, −1.14).

Solvation of lithiated formamide (1), acetamide (2), and *N*-methylacetamide (3): The preference for bridged *cis* structures in lithiated azaenolates (e.g., **1A**, **2A**, and **3A**) may be less pronounced if donor solvent molecules coordinate to the exposed lithium ion of the less stable *trans* forms. Reaction-field calculations[14] with a "continuum solvent" with the dielectric constant of THF change the relative energies of *cis* and *trans* forms completely. The bridged *cis* structure **1A** now has the same energy as the *trans* structures **1B** and **1C** (SCRF column in Table 1). In the acetamides **2** and **3**, however, the bulkier methyl groups give a larger cavity diameter in the calculations; the stabilization of the exposed, polar groups—NH, C=O, and Li^+—is therefore reduced, and the preference for the *cis* geometry is maintained in the SCRF calculations (Table 1). The geometry of the O-C-N moiety changes only slightly on going from the gas-phase calculation to the reaction-field environment (Table 2). However, the O–Li and N–Li bonds in the *trans* geometries (**1B**, **2B**, **3B** and **1C**, **2C**, **3C**) are stretched significantly (6–12 pm). This elongation is less pronounced in the *cis* structures **1A**, **2A**, and **3A**. The lithium ion still bridges O and N in the SCRF calculations of these structures.

Although continuum SCRF calculations might be useful in estimating the influence of solvents, they presumably do not take into account the different geometrical demands of solvent and solute. We therefore performed calculations for complexes of **1** with explicit dimethyl ether molecules as coordinating solvent (e.g., Fig. 5). The relative energies of the solvates of **1** with

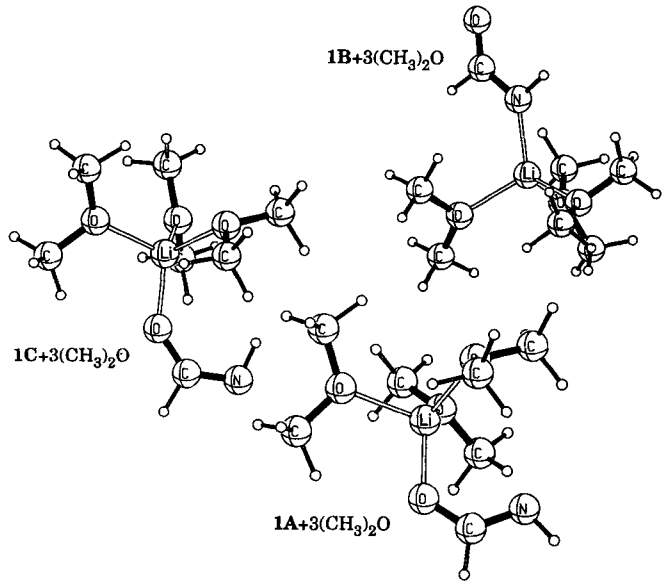

Fig. 5. Lithiated azaenolates of formamide solvated by three dimethyl ether molecules. The structures were optimized at HF/6-31 + G(d). See Table 1 for energies and Table 2 for geometrical parameters.

Table 2. Effect of Solvation on selected distances [a] in lithiated azaenolates.

Structure [b]	C–O [a]	C–N [a]	O–Li [a]	N-Li [a]
1A	126	130	185	192
1A(SCRF)	126	129	188	193
2A	127	131	183	191
2A(SCRF)	127	130	185	191
3A	127	131	182	191
3A(SCRF)	127	130	184	191
1B	122	134	[c]	180
1B(SCRF)	124	131	[c]	192
2B	122	134	[c]	180
2B(SCRF)	124	132	[c]	187
3B	122	134	[c]	180
3B(SCRF)	123	133	[c]	186
1C	129	127	163	[c]
1C(SCRF)	127	129	174	[c]
2C	130	127	163	[c]
2C(SCRF)	128	128	169	[c]
3C	129	128	170	[c]
3C(SCRF)	129	128	167	[c]
1A·Me_2O	126	130	188	195
1A·Me_2O(SCRF)	125	130	192	198
1B·Me_2O	121	133	[c]	183
1B·Me_2O(SCRF)	124	132	[c]	192
1C·Me_2O	129	127	165	[c]
1C·Me_2O(SCRF)	127	128	173	[c]
1A·3Me_2O	126	129	183	301
1A·3Me_2O(SCRF)	125	129	183	313
1B·3Me_2O	122	132	[c]	192
1B·3Me_2O(SCRF)	123	131	[c]	196
1C·3Me_2O	128	128	179	[c]
1C·3Me_2O(SCRF)	128	128	182	[c]

[a] Distances in pm optimized with the 6-31 + G(d) basis. [b] The structures are referenced in Table 1 and in Figures 2–5. They were optimized with and without a continuum reaction field with the dielectric constant of THF (SCRF column). [c] Lithium is not coordinated to the O or N atom respectively; the resulting large distance (> 300 pm) is not listed.

one, two, and three ether molecules are included in Table 1. Three dimethyl ether ligands stabilize the *trans* forms **1B**·3Me_2O and **1C**·3Me_2O very significantly, but the *cis* form **1A**·3Me_2O is still the global minimum at the 6-31 + G(d) level. The structure of the *cis*-azaenolate solvated by dimethyl ether differs significantly from that of the unsolvated molecule **1A**. In the solvate, the *cis* form looses the lithium bridge between O and N (Fig. 5, see also the Li–N bond lengths in Table 2). The four oxygen atoms can apparently only coordinate to the lithium ion when the latter is no longer coordinated to the nitrogen.

SCRF calculations on the complexes of **1** in Figure 5 give close to the same relative energies as those calculated by the SCRF model that does not explicitly include solvent molecules. However, the geometries of the reference structures **1A** and **1A**·Me_3O are quite different (see above, Tables 1 and 2). The calculations suggest that the continuum reaction field should not be used to predict the structure of ionic species unless a few specific solvent molecules are included in the system. Experimental data for the relative stabilities of the monomeric lithiated azaenolates are not available. Our calculations predict that both *cis* and *trans* structures should exist in an equilibrium mixture when an amide is deprotonated in donor solvents such as THF.

Barriers for the C–N rotation in azaenolates: When lithiated azaenolates are generated as synthetic intermediates in the modification of peptides, their geometry and rigidity will be important. Compound **1** can serve as a small model to explore the barrier to rotation about the C–N bond in azaenolates. The transformation of the most stable lithiated *trans*-azaenolate **1C** to the *cis*-azaenolate **1A** is depicted in Figure 6. The enolate passes through two transition states in the course of transforming the HCNH torsion angle from 180° in **1C** to 0° in **1A**.[15, 16]

0947-6539/96/0201-0012 $ 10.00+.25/0 Chem. Eur. J. 1996, 2, No. 1

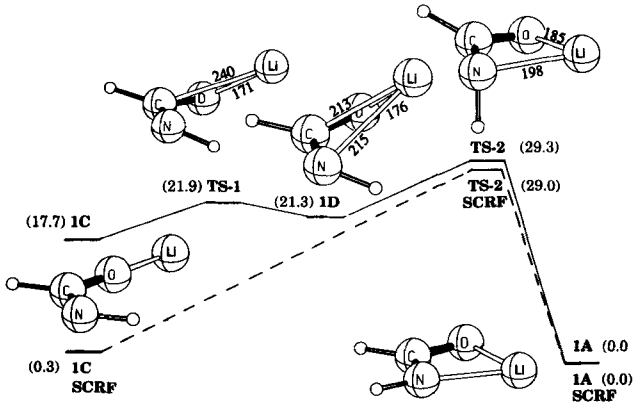

Fig. 6. The *cis*/*trans* isomerisation pathway for the lithiated azaenolate of formamide in the gas phase (solid line) and in the continuum solvent model (dashed line). The structures **1A**, **1C**, and **1D** are minima, and **TS-1** and **TS-2** are transition states on the potential energy surface. Relative energies are given in parentheses (kcal mol^{-1}; HF/6-31+G(d) and SCRF/6-31+G(d)). Geometry optimizations including electron correlation produce similar relative energies as that on the HF level (MP2/6-31+G(d) including zero-point energy correction: **1C**, 17.9; **TS-1**, 20.7; **1D**, 19.1; **TS-2**, 27.1; **1A**, 0.0 kcal mol^{-1}).

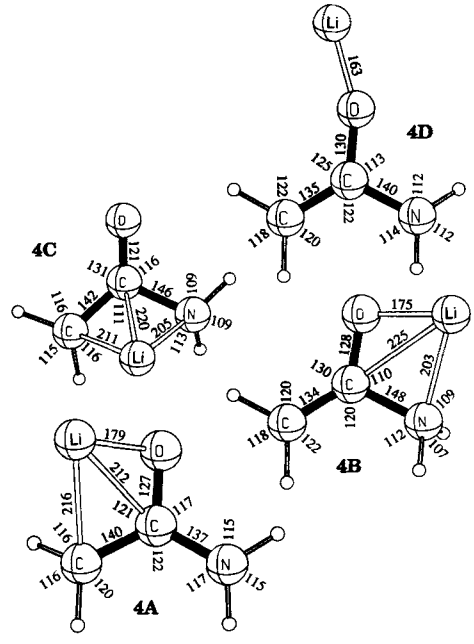

Fig. 7. Lithiated *C*-enolates **4A–D** of acetamide. See Table 1 for relative energies of these HF/6-31+G(d) structures. The form **4D** has C_s symmetry; the other structures have C_1 symmetry.

From coordinating only oxygen in **1C**, the lithium ion changes in the first transition state **TS-1** to binding both heteroatoms. The next intermediate, **1D**, resides in a shallow energy minimum. Here, the HCNH moiety is still only slightly twisted away from planarity (torsion angle = 167°). The second transition state (**TS-2**, torsion angle = 111°) determines the rate of rotation.

The situation changes when the solvation model is applied (see Fig. 6, dashed line). The structure **TS-2** remains the rate-determining barrier (now as **TS-2**(SCRF)). However, all attempts to locate an intermediate similar to **1D** fail. Starting at **TS-2**(SCRF), the intrinsic reaction coordinates[15] lead directly toward the minima **1A**(SCRF) and **1C**(SCRF), which now have approximately equal energy.

The results summarized in Figure 6 suggest that *trans*-azaenolate (**1C**) is kinetically stable when formed by deprotonation of the *trans* amide bonds of peptides in solution at low temperatures. The calculated barrier for the C–N bond rotation is high (ca. 28 kcal mol^{-1}), and it is reasonable to assume that temperatures above 0 °C are required to achieve isomerization within the time scale of a normal laboratory experiment. Recent reports on memory effects of heated solutions of azaenolates support this view: the product distribution is found to be different depending on whether sarcosine *C*-enolates embedded in a poly(azaenolate) peptide are alkylated directly at −75 °C or after a period of time at room temperature.[1b, 3]

Lithiated *C*-enolates of acetamide (4): Deprotonation of the NH_2 group in acetamide leads to the azaenolate anion; deprotonation at the α-carbon to the *C*-enolate. We calculate that the free (nonmetalated) *C*-enolate anion is ca. 18 kcal mol^{-1} less stable than the free azaenolate anion at the 6-31+G(d) level.[9] However, free anions are unlikely to exist in solution, the calculations depend on the size of the basis set, and correlation effects may be large. The present discussion is therefore restricted to different forms of the lithium salts of the *C*-enolate (**4**) and the azaenolate (**2**) of acetamide.

The lithium ion can coordinate to three basic sites in the *C*-enolate **4**: the nitrogen, the oxygen, and the CH_2 carbon. A systematic MNDO search of the conformational accessible positions for lithium yields four structures (**4A–D**). Their HF/6-31+G(d) optimized geometries are shown in Figure 7; the relative energies are included in Table 1. The α-carbon and the carbonyl oxygen chelate the lithium cation in **4A** very effectively. The alternative structure with N,O-coordination, **4B**, is less stable; to bind to the lithium ion, the NH_2 group can no longer adopt its favored orientation in a plane with the carbonyl group. The azaallyl structure **4C** is of even higher energy; the structure **4D**, with C_s symmetry, is a very unstable minimum on the energy surface.

Even the most stable of the lithiated *C*-enolates (**4A**) is too high in energy to be detected in equilibrium with the most stable azaenolate, **2A**. The preference for azaenolate structures is maintained when the reaction field is used to simulate the solvent (Table 1). It is therefore expected that peptides will be deprotonated at the amide group and not at the α-carbon if the experimental conditions allow a thermodynamic equilibration. The deprotonation experiments with peptides published so far[1, 2] support this assertion.

Dilithiated *N*-formylalaninamide (5) as model for a lithiated peptide: The "dipeptide models" *N*-acetylalanine-*N*′-methylamide or *N*-formylalaninamide (**12**) have been used extensively to calculate the conformational preferences of peptides at the dihedral angles ϕ and ψ. The results of such calculations are usually presented as Ramachandran diagrams of the form $E = f(\phi, \psi)$.[17] It is now generally accepted that ab initio calculations with large basis sets describe the conformational preferences of unsolvated small "dipeptides" correctly.[18] However, the conformations of large peptides, solvated peptides, and proteins are not reproduced by the small models.[18c, 19] In helices, pleated sheets, and loop regions of peptides, hydrogen

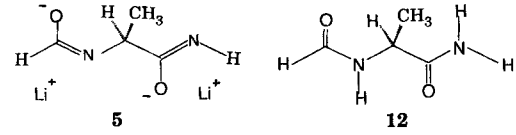

5 **12**

bonds between amino acids which are not close neighbors in the peptide chain are formed. Such hydrogen bonds cannot be formed in dipeptide models such as **12**. So, we expect that the different conformations and structures of dilithiated *N*-formylalaninamide **5**—the dilithiated derivative of **12**—will only model small lithiated peptides.

Search for stationary points on the conformational hypersurface: Compound **5** has two lithiated peptide bonds, which each can be "*cis*" or "*trans*". Four different forms of **5** must therefore be considered, namely, **5CC**, **5CT**, **5TC**, and **5TT**, where the first letter denotes the arrangement in the azaenolate derived from the *N*-formyl group and the second that in the azaenolate derived from the amide group (**C** = *cis* or **T** = *trans*).

The Ramachandran energy surfaces, $E(\phi, \psi)$, of all four forms of **5** were calculated semiempirically (MNDO[7]) to find conformational regions of low energy. The following procedure, exemplified with **5TT**, was used to locate low energy structures: conformations of **5** are expected to be stable when each azaenolate moiety in **5** has at least one contact to a lithium cation. Therefore, the distance of one lithium ion to O or N in the first enolate unit and that of the other lithium to O or N in the second enolate unit were kept fixed at the initial stage of the calculation of the Ramachandran maps. Four different energy surfaces with fixed Li–N and Li–O distances (205 pm) were initially calculated for **5TT** with MNDO. All other degrees of freedom (except ϕ and ψ) were optimized. The form of lowest energy was than selected at each ϕ/ψ combination. The right part (MNDO) of Figure 8 shows the surface of lowest energy obtained from combining all four initial surfaces. It is reasonably safe to assume that "real" low-energy structures are located close to the four minima of Figure 8. The four minimum geometries (**5TTa–d**) were reoptimized in all degrees of freedom by MNDO and ab initio methods (6-31+G(d)). The same procedure was used for the structures **5TC**, **5CT**, and **5CC**, which contain *cis* amide bonds.

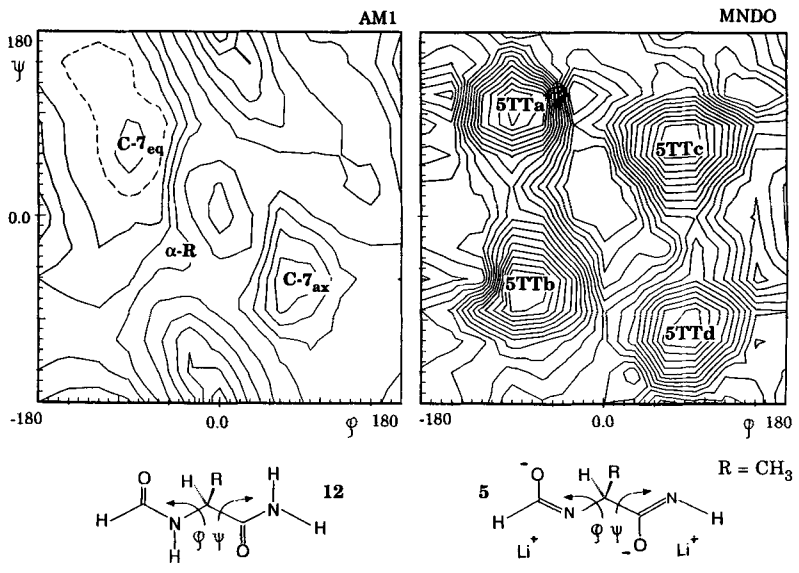

Fig. 8. Ramachandran maps of *N*-formylalaninamide (**12**), calculated with AM1, and corresponding graph of the lithiated derivative **5TT**, calculated with MNDO. The energy surface of **5TT** is a combination of four different maps with distinct lithium coordination (see text). The solid contour lines are spaced by 2 kcal mol^{-1} (dashed line 1 kcal mol^{-1}).

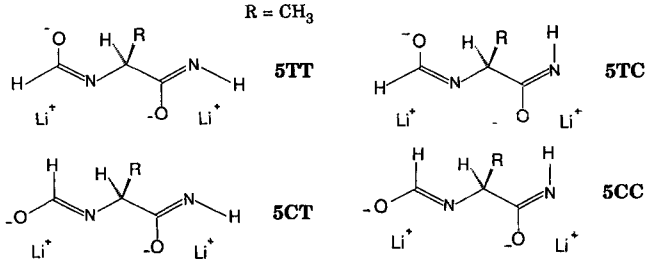

The Ramachandran diagram of the parent peptide (Fig. 8, left) is far less structured than the diagram of the corresponding lithiated compound. The strong electrostatic attraction between the lithium cations and the negatively charged O and N atoms dominates in **5TT**. Only four deep minima are conformationally allowed; their 6-31+G(d) structures are shown in the lower half of Figure 9. Of course, the Ramachandran diagrams in Figure 8 are only valid for the selected small model system. Long-range intramolecular interactions, possible in larger peptide systems, will open up additional conformationally allowed regions. Furthermore, aggregation and clustering with added ions and bases will change the energy surface. However, Ramachandran diagrams of small model peptides give the first insights into the structural diversity of lithiated peptides, hitherto unknown by experimental techniques.

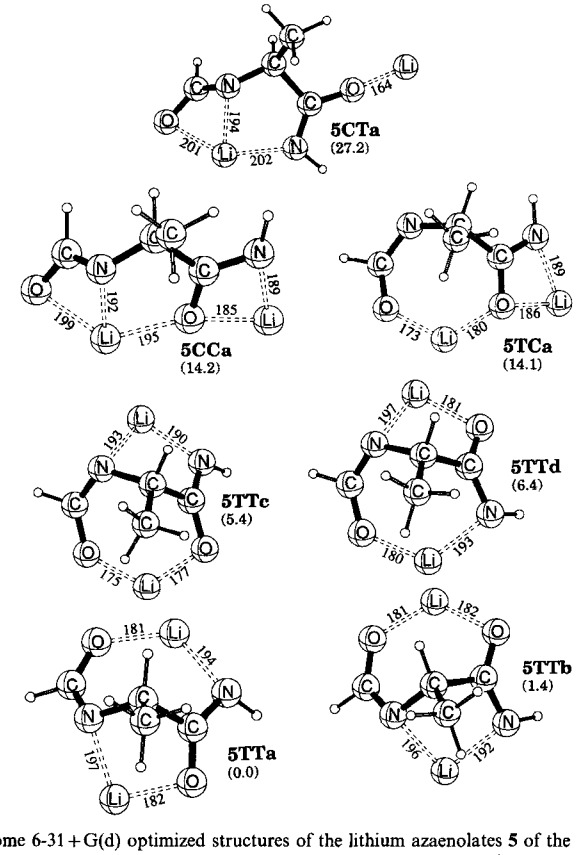

Fig. 9. Some 6-31+G(d) optimized structures of the lithium azaenolates **5** of the dipeptide model *N*-formylalaninamide. Relative energies (kcal mol^{-1}, HF/6-31+G(d)) are given in brackets. See Table 3 for further details.

Selected low-energy structures of **5**: The 6-31+G(d) low-energy structures of **5** are compiled in Table 3. The four minima of **5TT** and the structures of lowest energy found for **5CC**, **5TC**, and

0947-6539/96/0201-0014 $ 10.00+.25/0 Chem. Eur. J. 1996, 2, No. 1

Table 3. Relative energies (kcal mol^{-1}) of different geometries of dilithiated *N*-formylalaninamide (**5**) obtained by MNDO and ab initio calculations with the 6-31+G(d) basis. The dihedral angles ϕ and ψ of the peptide backbone are given in parentheses. Electron correlation is taken into account by using MP2(fc) single points on the 6-31+G(d) geometries. All structures were exposed to a continuum reaction field with the dielectric constant of THF and reoptimized to simulate solvation (SCRF column). Representative structures are shown in the Figure 9.

Structure	$H_{f(MNDO)}$ (ϕ, ψ)	$E_{6-31+G(d)}$ (ϕ, ψ)	E_{MP2} [a]	$E_{SCRF/6-31+G(d)}$ (ϕ, ψ)
5CCa	15.7 (−102, +173)	14.2 (−91, +178)	13.0	7.0 (−95, +180)
5CCb	18.1 (+113, +170)	17.5 (+102, +169)	16.6	10.1 (+102, +167)
5TCa	14.2 (+75, +89)	14.1 (+75, +100)	15.3	13.9 (+74, +103) [c]
5TCb	18.7 (−150, +153)	14.7 (−158, +160)	15.8	0.6 (−160, +160)
5CTa	26.4 (−100, +3)	27.2 (−93, −1)	26.0	4.2 (−156, −7) [d]
5CTb	28.9 (−59, −53) [b]	28.0 (−131, +5) [b]	26.7	1.4 (−159, −8)
5CTc	24.7 (+81, +21)	30.6 (+101, −7)	29.6	11.1 (+109, −11) [c]
5CTd	19.2 (−117, −53)	31.0 (−103, −155)	28.7	15.9 (−98, −170)
5CTe	22.5 (+90, −166)	35.0 (+82, −164)	32.9	18.6 (+103, +166)
5TTa	0.0 (−85, +111)	0.0 (−86, +114)	0.0	0.0 (−86, +114)
5TTb	−1.4 (−78, −68)	1.4 (−78, −61)	0.4	0.4 (−79, −60)
5TTc	2.5 (+74, +69)	5.4 (+69, +62)	4.4	4.4 (+69, +64)
5TTd	3.4 (+79, −111)	6.4 (+76, −113)	5.4	5.7 (+77, −113)

[a] MP2(fc)/6-31+G(d)//6-31+G(d). [b] The dihedral angles of this particular MNDO structure change significantly during the reoptimization by ab initio methods. The coordination sites of the lithium ions are however retained. [c] Upper limit, not yet fully converged. [d] The contact of one lithium ion to the formyl oxygen is lost in the SCRF optimization, so ϕ changed drastically.

5CT are reproduced in Figure 9. A perfect electrostatic stabilization is only possible in the all-*trans* forms (**5TT**). The *cis*-azaenolates, which are the most stable forms of the azaenolates of small amides (compounds **1A**, **2A**, and **3A**, see above), are less important structures in the azaenolate **5**. The four-membered chelate ring of these *cis* forms is only found in energetically unfavored structures as **5CCa**, **5CTa**, and **5TCa** (Fig. 9). The typical C_7 conformation, which is the most stable form of small dipeptide models such as **12**, resembles the minimum (**5TTa**) of the lithiated model **5**, but other structures (**5TTb–d**) are also very stable.

Solvation influences the relative energies of the different structures of **5**. We applied the same continuum solvation model, used for the smaller amides **1–4**, to the different structures of **5** (see Table 3). Application of the solvation model does not change the relative energies of the *trans* structures of **5** (**5TTa–d**) very much. Here, each lithium ion is already coordinated to one nitrogen and one oxygen, and none of the structures will gain significantly more energy than the others by solvation. However, some high-energy structures of **5** that contain exposed lithium ions are stabilized drastically in the continuum solvation model (e.g., **5CTa**, **5CTb**, and **5TCb** in Table 3, see also Fig. 9). More precise relative energies will be accessible with a first shell of specific solvent molecules (see the results above on the azaenolate **1** of formamide). However, such systems are at present too large to be handled in a high-level ab-initio study.

It is remarkable that the structures and energies calculated with MNDO come close to the ab initio data (with exceptions, such as **5CTb**). This is promising for future semiempirical calculations of large lithiated peptides such as lithiated cyclosporin A.[1]

Selected aggregates and lithium-bridged dimers: The discussion of solvation effects has already shown that the structures of lithiated amides and peptides change with the coordination sites available for the lithium cations. Aggregation is common in organolithium chemistry.[20a] However, the computational demands of calculations on large clusters are prohibitive. The current initial investigation is therefore restricted to two small aggregates, the dimer **14** of the *cis*-azaenolates of *N*-methylacetamide and the dimer **15** of the dilithiated *trans*-azaenolate of *N*-formylglycinaldehyde (Fig. 10). Compound **15** may serve as a small model that can adopt the arrangement of an antiparallel β-sheet. More complex structures including mixed aggregates[20b] are probably present when azaenolates of peptides are generated experimentally.

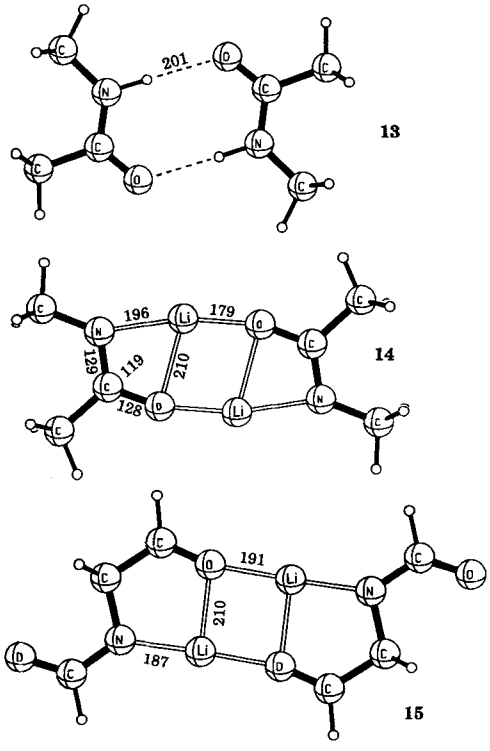

Fig. 10. Ab initio (6-31+G(d)) geometries of the dimers **14** and **15** of lithiated azaenolates. The structure of the dimer **13** of *cis*-*N*-methylacetamide is also given. The dimers **13** and **14** were optimized in C_2 and in C_i symmetry. Both types of calculations converged to the C_{2h} structures shown. Compound **15** was optimized with C_2 symmetric constraints and developed C_{2h} symmetry.

*Dimers of cis-N-methylacetamide (**13**) and of its lithiated azaenolate (**14**)*: The dimer **13** (Fig. 10) of *cis*-*N*-methylacetamide (*cis*-**11**, Fig. 4) contains many features that characterize hydrogen-bonded peptides. Two hydrogen bonds are formed in the head-to-tail arrangement, and the N···O separation is approximately 300 pm, as is observed in hydrogen-bonded peptide structures.[21] The dimerization energy is calculated to be 11.7 kcal mol^{-1} (HF/6-31 + G(d)), approximately twice the value expected for one hydrogen bond between peptides[11e, 22] (the energy is not corrected for basis set superposition errors[23, 24]).

Lithiation of **13** expands the structure; the N···O distance increases to ca. 370 pm in **14** (Fig. 10). The dimerization of **3A** to **14** is strongly exothermic (49.3 kcal mol^{-1}, HF/6-31+G(d)). The structure is similar to parts of the octameric lithium azaenolate complex formed by lithiated *N*-isopropylbenzamide in the solid state.[5b] The octameric complex can be regarded as being built up from four dimeric units similar to **14**. The mean C–O, C–N, Li–N, and Li–O bond lengths in the X-ray crystal structure are 131, 128, 200, and 220 pm, respectively, and are thus very close to the corresponding calculated distances in **14** (128, 129, 196, and 210 pm). The degree to which these values coincide is remarkable, if one considers the different substitution patterns and the higher lithium coordination in the octameric solid-state complex.

Dimer 15 of lithiated N-formylglycinaldehyde: The dimer **15** will reflect the structural changes that may occur in a β-sheet on lithiation. The most significant observation is that the N-Li-O net of **15**, formally replacing the N-H-O hydrogen bonds in a β-sheet, increases the distance between the α-carbons from approximately 500 pm in the β-sheet to 658 pm. The C_{2h} symmetry of **15** is reasonable with the achiral glycine as amino acid. Five-membered N-C-C-O-Li rings can be detected in **15** (Fig. 10). Such structures are already known from the model studies on the bis(azaenolate) of *N*-formylalaninamide (e.g, **5TTa**, Fig. 9).

NMR chemical shifts: NMR chemical shifts of the different forms of the azaenolates **1**–**3** and the bis(azaenolate) **5** were calculated with the gauge-including atomic orbital method (GIAO)[25a] using the 6-31G* basis on 6-31+G* geometries. Tables 4 and 5 list the absolute chemical shifts of oxygen, carbon, and nitrogen in the lithiated azaenolates and in their amide precursors. Figure 11 shows the increments in the shielding constants of oxygen and nitrogen that occur when the amide systems are lithiated. A few rules can be extracted from the data:

1) Deprotonation of amides to form lithiated azaenolates produces a shielding of the oxygen and a deshielding of the nitrogen atoms in all cases studied. The carbonyl C atoms are also deshielded, but less significantly.
2) Coordination of lithium ions to the oxygen of the azaenolates increases the shielding of the oxygen nucleus and the deshielding of the nitrogen (see of Fig. 11).
3) The chemical shifts of the carbonyl carbons are less sensitive to deprotonation (upfield shift increments between 3 and 30 ppm can be calculated from the data in Table 4 and 5). *cis*-Azaenolates may perhaps be detected by their relatively large shielding increment of 20–30 ppm, but exceptions to this rule should be noted (e.g., **5CTa** and **5CTc–e**). Only small upfield shift increments (3–11 ppm) are observed for *trans* structures when only one of the heteroatoms of the azaenolate moiety (O or N) coordinates to a lithium ion (in **1B–3B**, **1C–3C**, **5TCa**, **5TCb**, and **5CTa**).

Table 4. Calculated absolute isotropic NMR shielding of the amide oxygen, carbon, and nitrogen atoms in the amides **9**, **10**, and **11**, and in the different forms of the corresponding lithiated azaenolates (**1**, **2**, and **3**).

Structure	O	C	N
9	−34.8	47.9	185.0
1A	113.7	25.2	120.4
1B	−17.8	38.9	152.0
1C	184.3	45.0	67.7
1A·Me_2O	110.7	26.6	119.7
1A·2Me_2O	109.1	28.7	115.6
1A·3Me_2O	135.5	33.4	87.9
1B·Me_2O	−5.9	38.3	149.8
1B·2Me_2O	4.8	37.6	149.5
1B·3Me_2O	13.5	36.8	147.5
1C·Me_2O	178.7	43.7	73.1
1C·2Me_2O	164.3	41.9	79.9
1C·3Me_2O	151.2	38.4	86.1
10	−33.7	38.2	184.5
2A	120.4	16.1	119.6
2B	−14.4	29.8	147.0
2C	183.0	37.9	65.5
trans-**11**	−22.8	37.5	184.8
cis-**11**	−42.1	35.3	191.6
3A	103.4	16.1	132.0
3B	−13.2	32.0	145.0
3C	139.9	29.3	89.8

Table 5. Calculated absolute isotropic NMR shielding constants of the amide oxygens, carbons, and nitrogens, and of the C_α atom in *N*-formylalaninamide (**12**) and in the corresponding lithiated bis(azaenolate)s **5**.

Structure	O_{formyl}	C_{formyl}	$N_{alanine}$	C_α	$O_{alanine}$	$C_{alanine}$	N_{amide}
12 [a]	−12.3	44.9	163.0	159.9	−8.9	35.15	184.6
5CCa	62.7	27.9	106.3	149.8	165.0	5.0	120.7
5CCb	66.5	31.3	110.0	150.0	165.6	4.5	121.6
5TCa	138.8	38.97	90.8	145.6	194.1	10.9	106.7
5TCb	7.9	39.1	136.9	150.9	179.3	4.9	115.6
5CTa	67.5	29.5	103.2	148.6	174.7	17.4	104.7
5CTb	71.2	15.0	96.3	144.9	15.9	23.3	144.8
5CTc	70.9	32.9	106.3	150.2	176.2	16.8	104.5
5CTd	56.1	27.5	105.6	150.3	67.8	12.1	143.9
5CTe	47.8	30.9	109.6	151.9	61.4	14.1	146.3
5TTa	104.4	33.7	98.9	149.8	131.8	18.5	125.1
5TTb	104.9	33.5	93.6	148.5	94.1	14.4	137.0
5TTc	102.1	32.4	99.6	148.6	108.1	16.4	130.3
5TTd	98.9	32.7	107.3	147.2	112.1	19.6	127.8

[a] C-7_{eq} conformation.

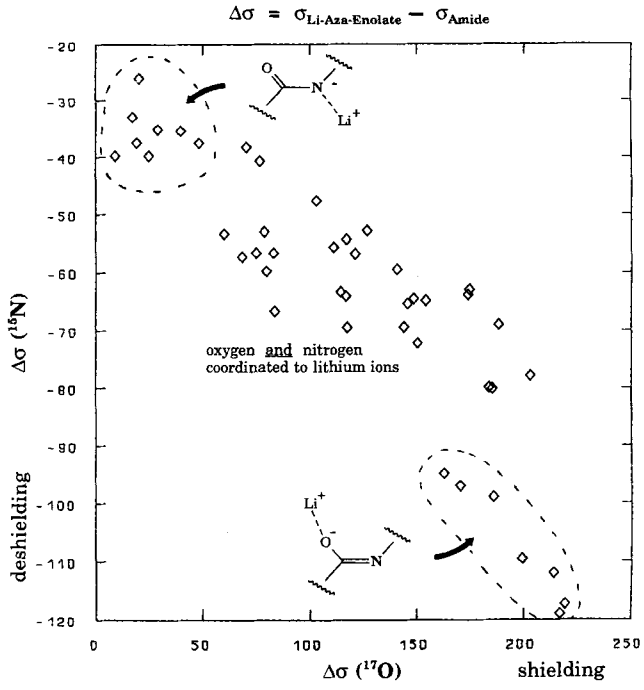

Fig. 11. Calculated changes $\Delta\sigma$ in the NMR shielding constants σ of oxygen and nitrogen when amides are converted to lithiated azaenolates. The data are shown for the azaenolates **1**, **2**, and **3**, for bis(azaenolate) **5**, and for their amide precursors **9**–**12**.

Conclusion

Lithiated azaenolates are reactive intermediates that can be formed from peptides. This computational study predicts some conformational rules for such systems:

1) Azaenolates and not *C*-enolates will be formed in peptides when the experimental conditions allow equilibration.
2) The four-membered chelate ring in the *cis*-azaenolate of amides (seen in the structures **1A**, **2A**, and **3A**) is exceptionally stable. Solvents may open the chelate, but the *cis* arrangement is still slightly favored compared to the *trans* structures **1B**, **2B**, **3B**, **1C**, **2C**, and **3C**.
3) The rotation about the C–N bond, which transforms the lithiated *trans*-azaenolate **1C** into the *cis* chelate **1A**, should

0947-6539/96/0201-0016 $ 10.00+.25/0 Chem. Eur. J. 1996, 2, No. 1

be more hindered than the corresponding rotational process in amides. Under kinetic control, *trans* peptide bonds can be deprotonated to *trans*-azaenolates. Equilibration by rotation about the C–N bond can only be achieved by warming the reaction mixture to temperatures above 0 °C, at which point isomerization rates become measurable.

4) Whereas isolated amides prefer the *cis* chelate, this rule does not always hold for peptides. Even the small peptide model **5** (the lithiated dipeptide model, *N*-formylalaninamide) coordinates the lithium ions in a complex manner. The most stable structure **5TTa** resembles a peptidic C_7 conformation, but other less common structures are also found.
5) Aggregates of lithiated peptides may show the overall shape of a peptidic β-sheet, but the distance between the peptide chains is increased.

This paper describes equilibrium structures of pure lithiated azaenolates. More complex systems, incorporating additional ionic salts, coordinating ligands, and co-solvents or quasi-dianion complexes,[26] will be investigated in future computational work. It is equally important to gain some understanding of the various dynamic processes in such complex systems to explain (and predict) the stereo- and regiochemistry of reactions in the presence of azaenolates.[27]

Computational Methods

For all azaenolates semiempirical (MNDO) [7] and ab initio calculations (with the Gaussian-92 program package [8]) were performed. Geometries were optimized with the HF/6-31+G(d) basis [28], which includes polarizing d functions at the heavy atoms augmented by diffuse functions. Symmetry restrictions were not imposed during the optimization. Often the calculations converge toward structures that contain symmetry elements (within numerical errors in the coordinates). The point group of such a symmetric structure is than given in the text or at the figures. Frequencies were calculated at the HF/6-31+G(d) level to ensure the nature of all stationary points and to derive vibrational corrections at 0 K (not scaled). The HF/6-31+G(d) structure was used as the basis for single-point Møller–Plesset (MP2(fc)) calculations [8,24,29] (Tables 1 and 3). In addition to this general procedure, geometry optimizations on correlated levels (MP2(fc) and (MP2(full)) with larger basis sets (up to 6-311+G(dp)) were carried out on the different isomers of the lithiated azaenolate **1**. The relative energies, calculated with the highest computational method used (MP4(fc)/6-311+G(d,p)//MP2(fc)/6-311+G(d,p)), come close to the relative energies calculated at the HF/6-31+G(d) level (see Fig. 1). The semiempirical MNDO [7] or AM1 [30] calculations were carried out using the VAMP4.5 [31] or MOPAC6.0 [32] program packages. NMR chemical shifts were predicted with the gauge-including atomic orbital method [25a] implemented into the Turbomol program package [25b,c] using a 6-31G(d) basis on the 6-31+G(d) geometries.

Acknowledgment: We thank the Deutsche Forschungsgemeinschaft and the Fonds der Chemischen Industrie for financial support. W. H. B. S. thanks the Studienstiftung des Deutschen Volkes for a fellowship.

Received: April 18, 1995 [F121]

[1] a) D. Seebach, A. K. Beck, H. G. Bossler, C. Gerber, S. Y. Ko, C. W. Murtiashaw, R. Neaf, S. Shoda, A. Thaler, M. Krieger, R. Wenger, *Helv. Chim. Acta* **1993**, *76*, 1564–1590. b) H. G. Bossler, D. Seebach, *ibid.* **1994**, *77*, 1124–1165.

[2] a) D. Seebach, *Aldrichimica Acta* **1992**, *25*, 59–66. b) D. Seebach, *Angew. Chem.* **1988**, *100*, 1685–1715; *Angew. Chem. Int. Ed. Engl.* **1988**, *27*, 1624–1654. c) D. Seebach, H. Bossler, H. Gründler, S. Shoda, R. Wenger, *Helv. Chim. Acta* **1991**, *74*, 197–224. d) S. A. Miller, S. L. Griffiths, D. Seebach, *ibid.* **1993**, *76*, 563–595.

[3] For a comprehensive review, see: D. Seebach, A. K. Beck, A. Studer, in *Modern Synthetic Methods, Vol. 7* (Eds.: B. Ernst, C. Leumann), VHCH/VCH, Basel/Weinheim **1995**, p. 1–178.

[4] K. W. Aston, L. H. Susan, A. S. Modak, D. P. Riley, K. R. Sample, R. H. Weiss, W. L. Neumann, *Tetrahedron Lett.* **1994**, *35*, 3687–3690.

[5] a) T. Maetzke, C. P. Hidber, D. Seebach, *J. Am. Chem. Soc.* **1990**, *112*, 8248–8250. b) T. Maetzke, D. Seebach, *Organometallics* **1990**, *9*, 3032–3037. c) G. Boche, C. Boie, F. Bosold, K. Harms, M. Marsch, *Angew. Chem.* **1994**, *106*, 90–91; *Angew. Chem. Int. Ed. Engl.* 115–117.

[6] For structural related compounds see for example: a) P. v. R. Schleyer, *Pure Appl. Chem.* **1983**, 355–362. b) R. D. Bach, M. L. Braden, G. J. Wolber, *J. Org. Chem.* **1983**, *48*, 1509–1514. c) M. L. McKee, *J. Am. Chem. Soc.* **1985**, *107*, 7284–7290. d) L. J. Bartolotti, R. E. Gawley, *J. Org. Chem.* **1989**, *54*, 2980–2982.

[7] M. J. S. Dewar, W. Thiel, *J. Am. Chem. Soc.* **1977**, *99*, 4899–4907.

[8] Gaussian 92/DFT, Revision F.2; M. J. Frisch, G. W. Trucks, H. B. Schlegel, P. M. W. Gill, B. G. Johnson, M. W. Wong, J. B. Foresman, M. A. Robb, M. Head-Gordon, E. S. Replogle, R. Gomperts, J. L. Andres, K. Raghavachari, J. S. Binkley, C. Gonzalez, R. L. Martin, D. J. Fox, D. J. Defrees, J. Baker, J. J. P. Stewart, J. A. Pople, Gaussian, Pittsburgh PA, **1993**.

[9] The following relative energies were calculated for the anions that result when acetamide is deprotonated: (6-31+G(d); MP2(fc)/6-31+G(d)//6-31+G(d); MP2 calculation corrected by zero-point energies). Azaenolate (CH_3,H-*trans*): 0.0; 0.0; 0.0 kcal mol^{-1}. Azaenolate (CH_3,H-*cis*): 6.5; 6.3; 6.1 kcal mol^{-1}. *C*-enolate: 17.8; 19.1; 18.6 kcal mol^{-1}.

[10] Recent ab initio calculations on formamide **9** [11a,b], the formamide enole *cis*-**6** [11b,c], acetamide **10** [11d], and *cis* [11e] and *trans* [11f–h] *N*-methylacetamide **11** with high-level basis sets give similar geometries (note, however: the most stable conformers of **10** and *cis*-**11** have C_1 symmetry optimized at the HF/6-31+G(d) level (not C_s)—the barriers for rotation of the methyl groups are very small (e.g., 0.03 kcal mol^{-1} for acetamide). Formamide has C_s symmetry in our HF/6-31+G(d) calculations, whereas a C_1-symmetric structure with a slightly nonplanar amide function is the minimum at correlated levels [11a,11b,12].

[11] a) M.-C. Ou, M.-S. Tsai, S.-Y. Chu, *J. Mol. Struct.* **1994**, *310*, 247–254. b) J. S. Kwiatkowski, J. Leszczynski, *J. Mol. Struct.* **1992**, *270*, 67. c) M. W. Wong, K. B. Wiberg, M. Frisch, *J. Am. Chem. Soc.* **1992**, *114*, 1645–1652. d) S. Tsuzuki, K. Tanabe, *J. Chem. Soc. Perkin Trans. 2* **1991** (8), 1255–1260. e) H. Guo, M. Karplus, *J. Phys. Chem.* **1992**, *96*, 7273–7287. f) N. G. Mirkin, S. Krimm, *J. Mol. Struct.* **1991**, *236*, 97–111. g) N. G. Mirkin, S. Krimm, *J. Am. Chem. Soc.* **1990**, *112*, 9016–9017. h) W. L. Jorgensen, J. Gao, *ibid.* **1988**, *110*, 4212–4216.

[12] HF/6-31+G(d) geometry optimizations presumably underestimate the nonplanarity of NH_2 groups, see, for example: J. Sponer, P. Hobza, *J. Am. Chem. Soc.* **1994**, *116*, 709–714, and references therein.

[13] a) A. E. Reed, R. B. Weinstock, F. Weinhold, *J. Chem. Phys.* **1985**, *83*, 735–746. b) A. E. Reed, L. A. Curtiss, F. Weinhold, *Chem. Rev.* **1988**, *88*, 899–926.

[14] a) L. Onsager, *J. Am. Chem. Soc.* **1936**, *58*, 1486–1493. b) M. W. Wong, M. J. Frisch, K. B. Wiberg, *ibid.* **1991**, *113*, 4776–4782.

[15] Intrinsic reaction coordinates were calculated on this rotational pathway, see: C. Gonzales, H. B. Schlegel, *J. Chem. Phys.* **1989**, *90*, 2154–2161; J. *Phys. Chem.* **1990**, *94*, 5523–5527.

[16] All Attempts failed to find a transition state for the transformation of **1C** to **1A** with conservation of the C_s symmetry. A stationary point found in this nitrogen-inversion pathway has two imaginary frequencies and is of very high energy (E_{rel} = 40.1 kcal mol^{-1}, HF/6-31+G(d)).

[17] a) G. N. Ramachandran, V. Sasisekharan, *Adv. Prot. Chem.* **1968**, *23*, 283–438 b) A. Perczel, J. G. Angyan, M. Kajtar, W. Viviani, J.-L. Rivail, J.-F. Marcoccia, I. G. Csizmadia, *J. Am. Chem. Soc.* **1991**, *113*, 6256–6265.

[18] See for example: a) T. Head-Gordon, M. Head-Gordon, M. J. Frisch, C. L. Brooks, J. A. Pople, *J. Am. Chem. Soc.* **1991**, *113*, 5989–5997. b) H.-J. Böhm, S. Brode, *ibid.* **1991**, *113*, 7129–7135. c) L. Schäfer, S. Q. Newton, M. Cao, A. Peeters, C. Van Alsenoy, K. Wolinski, F. A. Momany, *ibid.* **1993**, *115*, 272–280.

[19] a) A. Perczel, M. A. McAllister, P. Csaszar, I. G. Csizmadia, *J. Am. Chem. Soc.* **1993**, *115*, 4849–4858. b) H. S. Shang, T. Head-Gordon, *ibid.* **1994**, *116*, 1528–1532 c) A. Perczel, Ö. Farkas, I. G. Csizmadia, *ibid.* **1995**, *117*, 1653–1654.

[20] a) For leading references to the structures of organolithium systems, see: W. N. Setzer, P. v. R. Schleyer, *Adv. Organomet. Chem.* **1985**, *24*, 353–451. b) For the synthetic use of aggregation in enolate chemistry, see: E. Juaristi, A. K. Beck, J. Hansen, T. Matt, T. Mukhopadhyay, M. Simson, D. Seebach, *Synthesis* **1993**, 1271–1290.

[21] a) J. S. Richardson, *Adv. Prot. Chem.* **1981**, *34*, 167–339. b) K.-C. Chou, G. Nemethy, G.; H. A. Scheraga, *Acc. Chem. Res.* **1990**, *23*, 134–141. c) G. A. Jeffrey, W. Saenger, *Hydrogen Bonding in Biological Structures*, Springer: Berlin, 1991. d) J. Bernstein, C. Etter, L. Leiserowitz, *The Role of Hydrogen Bonding in Molecular Assemblies*, Structure Correlation, Vol. 2 (Eds.: H.-B. Bürgi, J. D. Dunitz), VCH: New York, **1994**.

[22] a) J. J. Novoa, M.-H. Whangbo, *J. Am. Chem. Soc.* **1991**, *113*, 9017–9026. b) M. Aida, *Bull. Chem. Soc. Jpn.* **1993**, *66*, 3423–3429.

[23] E. Clementi, *Computational Aspects for Large Chemical Systems*, Lecture Notes in Chemistry, Vol. 19.; Springer, New York, **1980**.

[24] W. J. Hehre, L. Radom, P. v. R. Schleyer, J. A. Pople, *Ab initio Molecular Orbital Theory*, John Wiley: New York, **1986**.

[25] a) R. Ditchfield, *Mol. Phys.* **1974**, *27*, 789–807. b) R. Ahlrichs, M. Bär, M. Häser, H. Horn, C. Kölmel, *Chem. Phys. Lett.* **1989**, *162*, 165–169. c) Turbomol, version 2. 3. San Diego: Biosym Techn. **1993**.

[26] W. Zarges, M. Marsch, K. Harms, G. Boche, *Angew. Chem.* **1989**, *101*, 1424–1425; *Angew. Chem. Int. Ed. Engl.* **1989**, *28*, 1392–1393.
[27] See for example the replacement of diastereotopic sarcosine protons in the hexalithio derivative of cyclosporine A; discussed on pp. 130–138 in ref. [3].
[28] a) J. Chandrasekhar, J. G. Andrade, P. v. R. Schleyer, *J. Am. Chem. Soc.* **1981**, *103*, 5609–5612. b) G. W. Spitznagel, T. Clark, J. Chandrasekhar, P. v. R. Schleyer, *J. Comput. Chem.* **1982**, *3*, 363–371. c) J. Kaneti, P. v. R. Schleyer, T. Clark, J. A. Kos, G. W. Spitznagel, J. G. Andrade, J. B. Moffat, *J. Am. Chem. Soc.* **1986**, *108*, 1481–1492.
[29] a) C. Møller, M. S. Plesset, *Phys. Rev.* **1934**, *46*, 618–622. b) J. S. Binkley, J. A. Pople, *Int. J. Quantum Chem.* **1975**, *9*, 229–236. c) M. J. Frisch, R. Krishnan, J. A. Pople, *Chem. Phys. Lett.* **1980**, *75*, 66–68.
[30] M. J. S. Dewar, E. G. Zoebisch, E. F. Healy, J. J. P. Stewart, *J. Am. Chem. Soc.* **1985**, *107*, 3902–3909.
[31] VAMP 4.5; T. Clark, G. Rauhut, J. Chandrasekhar, University of Erlangen-Nürnberg, 1993.
[32] MOPAC 5.0/6.0; J. J. P. Stewart, QCPE Program No. 455, Indiana University, Bloomington, Indiana.

0947-6539/96/0201-0018 $ 10.00+.25/0